High-pressure high-temperature behavior of polymer derived amorphous B-C-N

Shrikant Bhat[1*], Stefan Lauterbach[1], Dmytro Dzivenko[1], Christian Lathe[2], Lkhamsuren Bayarjargal[3], Marcus Schwarz[4], Hans-Joachim Kleebe[1], Edwin Kroke[4], Björn Winkler[3] and Ralf Riedel[1]

[1] FB Material- und Geowissenschaften, Technische Universität Darmstadt, Darmstadt, Germany
[2] Geoforschungszentrum (GFZ), Potsdam, Germany
[3] Institut für Geowissenschaften, Goethe-Universität Frankfurt, Frankfurt am Main, Germany
[4] Institut für Anorganische Chemie, TU-Bergakademie Freiberg, Freiberg, Germany

* Author to whom correspondence should be addressed; bhat@materials.tu-darmstadt.de

Abstract: Dense diamond-like BCN compounds are of interest due to their extreme hardness and predicted excellent thermal and chemical stability, which are superior to those of diamond and c-BN. Here, we report on the high-pressure high-temperature (HP-HT) behavior of amorphous BC_2N and BC_4N –as potential precursors for HP-HT synthesis of diamond-like BCN. Prepared via hydroboration reaction of piperazine borane and pyridine borane, respectively, amorphous BC_2N and BC_4N are characterized by well-mixed B-N, C-C and C-N bonds, confirmed by XPS analysis. These BCN compositions were subjected to pressures between 5-12 GPa and temperatures up to 1700 °C using multi-anvil apparatus and toroid-type press. In- and ex-situ X-ray diffraction reveals the decomposition of BC_4N to graphite and h-BN between 5 and 12 GPa above 500 °C, in contrast to BC_2N which remains amorphous up to 1600 °C.

1. Introduction

Dense B-C-N ternary phases have drawn considerable attention during last two decades due to their predicted properties, making them the best alternative to diamond and c-BN [1]: Super-hard BCN phase is believed to be harder than c-BN and to have better thermal and oxidation stability than diamond [1, 2]. Moreover, a variety of attracting properties were reported recently for BCN nano-structures: enhanced lithium storage capability for battery application [2], compositionally tunable electronic properties [3], photo-luminescence [4] and hydrogen storage properties [5-7]. Many efforts were undertaken to achieve crystalline ternary BCN under high-pressure high-temperature (HP-HT) conditions. HP-HT experimental studies on BCN were initiated by Badzian et al. [8], who reported formation of mixed crystals of c-BN and diamond. Subsequent HP-HT studies can be roughly divided into two categories: i) Synthesis at 20 GPa and above, focusing on superhard cubic B-C-N phase; ii) synthesis below 20 GPa, focusing on crystalline graphitic ternary B-C-N. As our experiments above 20 GPa will be discussed elsewhere, this article is focused on the HP-HT behavior of amorphous B-C-N precursors below 20 GPa.

With respect to the previous studies of B-C-Ns below 20 GPa, Nakano et al. [9] and Sasaki et al. [10] subjected graphitic BC_2N to 7.7 GPa, 2000-2400 °C and 5.5 GPa, 1400-1600 °C (with Co-catalyst), respectively, and indicated phase separation into cubic boron nitride and diamond. Later Solozhenko et al. [11] studied graphite-like BC_4N up to 1800 °C and 7 GPa using multi anvil press and showed its metastable behavior. Nicolich et al. [12] reported the formation of ordered graphitic ternary crystals from turbostratic BCN around 3-5 GPa and 1200-1500 °C. Hexagonal BCN (h-BCN) was obtained by Tian et al. [13] at 5.5 GPa and 1600 °C using $Ca_3B_2N_4$ catalyst. Several recent papers reported formation of h-BCN [14], orthorhombic $BC_{3.3}N$ [15], solid solutions of c-BN in carbon [16], and even c-BCN below 20 GPa and 2000 °C [17-19]. However, the reported results are rather contradictory and neither provide clear evidence of the single BCN phase nor give unambiguous structural and compositional information.

In the present paper we report on the HP-HT behavior of amorphous BC_2N and BC_4N, which are synthesized via hydroboration reaction of piperazine borane and pyridine borane, respectively [1, 20, 21]. The HP-HT experiments between 5 and 12 GPa and up to 1700 °C were realized using multi anvil and toroid-type presses. The samples were characterized by *in* and *ex–situ* X-ray diffraction (XRD).
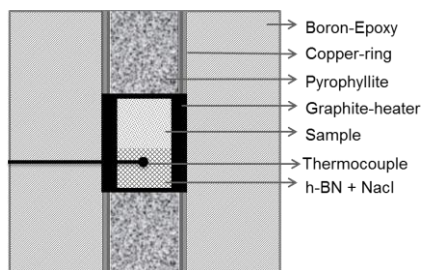
2. Experimental

2.1. In-situ synthesis in multi-anvil (MAX80) press
In-situ HP-HT energy-dispersive X-ray powder-diffraction (EDXRD) experiments were performed in a cubic multi-anvil apparatus, MAX-80, installed at the F2.1 beamline at Hasylab (DESY, Hamburg). A few milligrams of samples were loaded into a graphite cylinder, serving as sample chamber as well as resistance heater in the middle of a boron-epoxy cube. A mixture of NaCl/h-BN for pressure calibration was placed above and below the sample in the cylinder. The sample was separated from the pressure standard with a thin layer of h-BN. The cubic cell was located between six tungsten carbide anvils driven by the large hydraulic press. Electric current was sent through the graphite heater via two opposite anvils. The temperature was measured with a Pt10%Rh-Pt thermocouple, inserted perpendicularly to the axis of the furnace in the h-BN layer above the sample. Actual pressure applied to the samples was calculated from the equation of state of NaCl [22]. The 8 mm and 6 mm cubes were used for experiments up to 5 GPa and 7 GPa, respectively. The schematic diagram of the cube is given in figure 1**.** Samples were heated up to 1700 °C in steps of 100 °C/min and EDXRD patterns were collected at every step. After the desired temperature was reached, samples were quenched by turning off the electric current, and the sample cube was recovered after slow decompression. EDXRD was collected by using a white beam with a spot size of 0.7 mm in the energy range 2-80 keV and a high purity Ge solid state detector fixed at the diffraction angle $2\theta = 9.03°$. The diffraction angle was calculated from NaCl spectra taken at ambient pressure. In the figures, the EDXRD data were plotted as intensity vs. 2θ (by fixing $\lambda = 0.70931$ Å) for the sake of comparison with other XRD data.
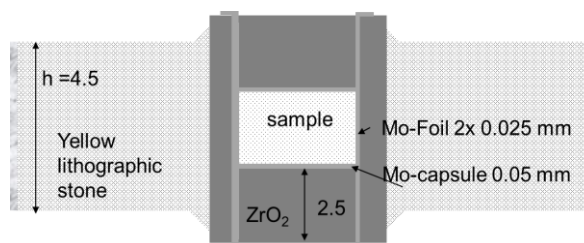
2.2. Toroid experiments
Synthesis in the toroid-type press was carried out using a 8.5 mm toroidal pressure cell with a lithographic limestone gasket [23]. The starting amorphous BC_2N and BC_4N powders were loaded into 2.8 mm outside diameter, 0.05 mm wall thickness, and 2.5 mm length molybdenum (Mo) foil capsules and pre-compressed in a metal die. The capsule was inserted into the middle of the Mo cylinder of 7.5 mm in height and 0.0025 mm in thickness, serving as heating chamber. The rest of the volume in the cylinder was filled by zirconium oxide plungers. The schematic diagram of the cell is given in figure 2. The pressure-versus-ram load relation of the device has been calibrated using phase transformations of Bi at 2.55 and 7.7 GPa at room temperature, in combination with the general shape of the pressure-load curve of these devices [23]. The temperature was estimated from the applied electric power using the spontaneous nucleation of diamond from Ni-Mn-Graphite (~1500°C) [24] and sintering of α-Si_3N_4 powder as reference points. After compression to ~ 12.0 GPa at room temperature, the samples were

heated up to the target power level (corresponding to T = 1000-1100 °C) which was kept for 5 min. Then, the samples were quenched to room temperature before the pressure was released.

Figure 1. The schematic diagram of the cube used in multi-anvil (Max-80) experiments.

Figure 2. The schematic diagram of the cell used in toroid-type experiments.

After the experiments, the capsules containing HP/HT-treated samples were recovered by cutting the cube/cell with a diamond disc. Then the graphite- and Mo- capsules were broken by using a diamond wire saw and a hard metal tool, respectively. The quenched samples were extracted and ground in a mortar to obtain a fine powder for subsequent characterization.

2.3 Characterization
The carbon (C), nitrogen and oxygen (N & O) content in BC_2N and BC_4N precursors were determined by combustion analysis using LECO C-200 and LECO TC-436, respectively. Angle-dispersive X-ray powder diffraction data were collected in capillary-sample transmission geometry (HP/HT-treated samples) and flat-sample transmission geometry (starting specimens) on a STOE STADI P diffractometer with Mo-Kα1 (λ= 0.70931 Å) radiation with a position-sensitive detector having 6° aperture. XPS investigations were carried out in PHI-VersaProbe-II using monochromatic Al-Kα (1486.6 eV) radiation as a photon excitation source.

3. Results and Discussion

3.1. Precursor synthesis and characterization
The precursors BC_2N and BC_4N were prepared by the hydroboration reaction of piperazine borane and pyridine borane, respectively [1, 20]. Bulk elemental analyses results of C, N and O contents of precursors are given in table 1. Each sample is analyzed by taking 5 random specimens. The results indicate that samples are homogeneous with less standard deviation. The C to N ratio of precursors (1.85 and 3.97), confirm the empirical formula BC_2N and BC_4N. The minor amount of oxygen of 2.4 and 1 wt% observed in BC_2N and BC_4N, respectively, is due to the surface absorption.

Table 1. Bulk elemental analyses results of the BCN precursors.

C [wt %]	**N** [wt %]	**O** [wt %]	Empirical Formula
45.7±0.9	29.17±1.8	2.41±0.2	$BC_{1.85}N_{1.01}O_{0.08}$ ~ **BC_2N**
65.5±1.3	18.32±1.7	0.95±0.25	$BC_{3.97}N_{0.95}O_{0.04}$ ~ **BC_4N**

XRD patterns of the precursors are shown in figure 3, indicating the amorphous nature of both BC_2N and BC_4N. The broad reflections observed in the diffraction patterns (marked with *) can be due to the turbostratic nature of the BCN coming from the (002) and (10) reflections similar to h-BN and

graphite [21, 25, 26]. XPS analysis results for precursors are listed in table 2 with B1s, C1s and N1s energies (in eV) assigned to particular type of bonding.

Table 2. XPS peak analysis results of precursors.
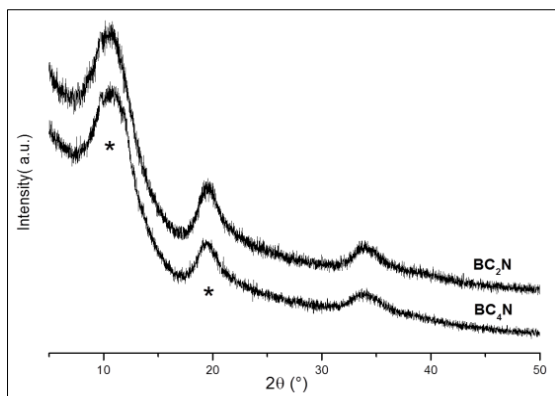
Figure 3. XRD patterns of precursors.

	BC_2N	BC_4N
C 1s	Position (eV)	Position (eV)
C-C	284.6	284.7
C-N	285.9	286.1
C-O/C=O	287.1	-
N 1s		
N-B	398.4	398.3
N-C	399.6	399.7
B 1s		
B-N-C	192.2	191.9
B-N	190.9	190.5

XPS results confirm the presence of C-C, C-N, N-C, N-B, B-N and B-N-C [27, 28] bondings as well as indicate the presence of C-O or C=O bondings in BC_2N due to surface absorbed oxygen (2.4%), which was also revealed by elemental analysis. Estimation of the intensity ratios of the different bonding energies indicates high amount of C-C and B-N type bonding; however, the presence of noticeable amount of N-C, C-N [29] and B-N-C [27] bonds is also unambiguous. In contrast, the B-C bondings were not observed in both precursors.

3.2. Results of In-situ Multi-Anvil and Toroid experiments

In-situ XRD patterns for BC_2N at 5 GPa and BC_4N at 7 GPa are shown in figures 4 and 5 respectively. The main intense peak (marked) is related to the graphite heater surrounding the sample. The samples exhibit the broad reflections which are similar to those measured *ex-situ* on the starting material (see figure 3). As one of the broad reflections (at 2θ ~10°) is over lapping the (002) graphite reflection from heater, the other broad regions give a hint about the samples under HP-HT conditions. From the figures 4 and 5 it can be seen that BC_2N and BC_4N remain amorphous up to 1500 °C and 500 °C, respectively. During further heating at a given pressure, a new peak (around 2θ ~ 20°) started to appear at 1600 °C and 600 °C for BC_2N and BC_4N, respectively. The corresponding insets in figures 4 and 5 give a closer look on the 2θ-region from 15 ° to 35 °, where the new sharp reflection can be clearly seen. *Ex-situ* XRD patterns of the quenched and recovered BC_2N and BC_4N samples are shown in figure 6. Both samples show crystalline nature with reflections indicating a mixture of h-BN and graphite. It is apparent that both BC_2N and BC_4N tend to decompose into a mixture of h-BN and graphite under the chosen HP-HT conditions.
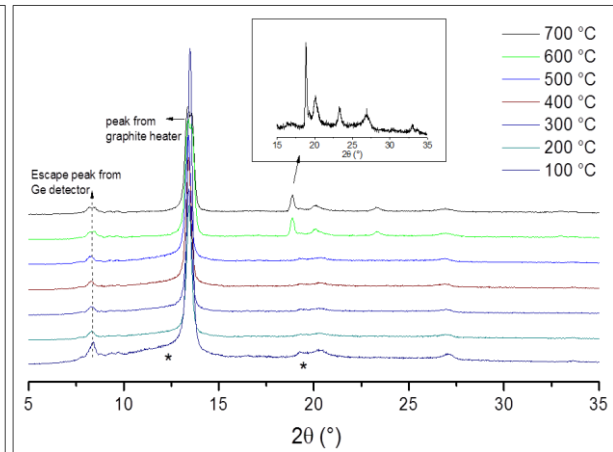
XRD patterns of the recovered samples from the toroid experiments at 12 GPa and ~ 1000°C are shown in figure 7. They show that BC_2N remains amorphous even after exposing to HP-HT conditions, whereas BC_4N decomposes into h-BN and graphite. The additional reflections were assigned to molybdenum carbides (Mo_2C and MoC), thus indicating that the molybdenum capsule reacted with the part of the sample. The results of *ex-situ* toroid experiments are in agreement with the above described *in-situ* multi-anvil studies, where BC_4N decomposed into h-BN and graphite at temperature exceeding 500 °C. Similarly, BC_2N has been found to maintain its amorphous nature up to 1600 °C at 5 GPa in multi-anvil and up to ~ 1100 °C at 12 GPa in the toroid experiment.

4. Conclusions

We have synthesized polymer derived ceramic precursors BC_2N and BC_4N having predefined bondings, which are also amorphous in nature. Our high pressure experiments (5-12 GPa) indicate that BC_4N decomposes to h-BN and graphite at temperatures above 500 °C, whereas BC_2N remains amorphous up to 1600 °C at 5 GPa and up to 1100 °C at 12 GPa.
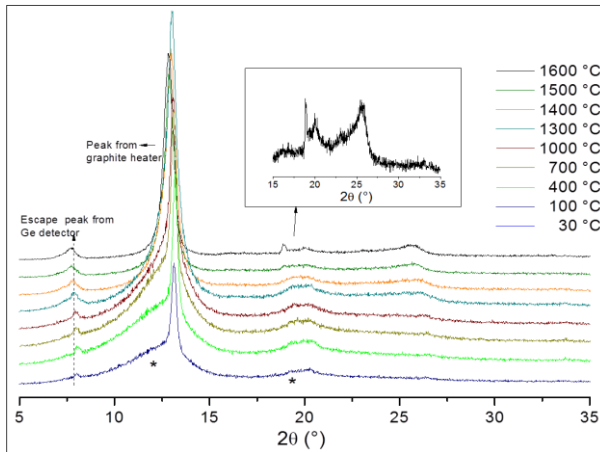

Figure 4. *In-situ* XRD patterns for BC_2N taken at 5 GPa in Max-80; inset graph shows a magnification of the 2θ region from 15 to 35 ° for the pattern taken at 1600 °C.

Figure 5. *In-situ* XRD patterns for BC_4N taken at 7 GPa in Max-80; inset graph shows a magnification of the 2θ region from 15 to 35 ° for the pattern taken at 700 °C.
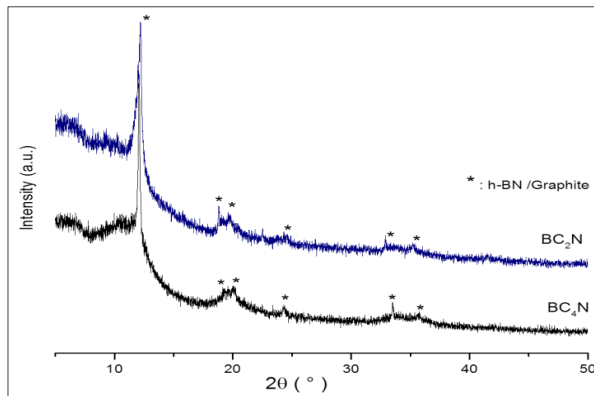
Figure 6. *Ex-situ* XRD patterns of the samples recovered after Max-80 experiments.
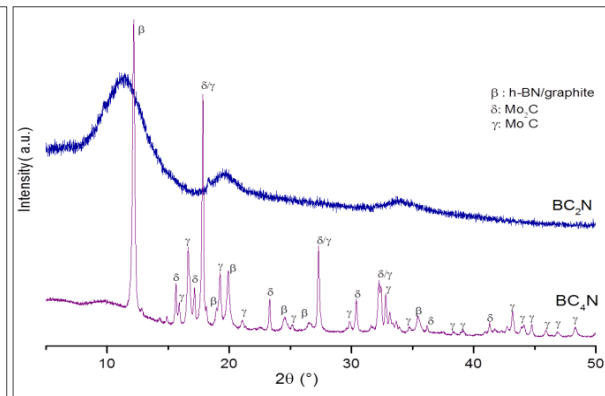
Figure 7. *Ex-situ* XRD patterns of the samples recovered after toroid experiments.

In order to achieve crystalline ternary phases in the B-C-N system one may need to investigate the behavior of these precursors at pressures exceeding 15 GPa. As both precursors tend to convert into mixtures of thermodynamically stable phases like h-BN and graphite, systematic kinetic studies at high pressure (e.g., upon variation of the heating time and temperature) are necessary in order to evaluate the formability of ternary B-C-N phases in future HP-HT experiments.

References

[1]   Riedel R 1992 *Adv. Mater.* **4** 759-761
[2]   Lei W W, Qin S, Liu D, Portehault D, Liu Z W and Chen Y 2013 *Chem. Commun.* **49** 352-354
[3]   Ci Li, Song L, Jin C, Jariwala D, Wu D, Li Y, Srivastava A, Wang Z F, Storr K, Balicas L, Liu F and Ajayan P M 2010 *Nature Mater.* **9** 430-435
[4]   Lei W, Portehault D, Dimova R and Antonietti M 2011 *J. Am. Chem. Soc.* **133** 7121-7127
[5]   Bhattacharya S, Majumder C and Das G P 2008 *J. Phys. Chem.* C **112** 17487-91
[6]   Portehault D, Giordano C, Gervais C, Senkovska I, Kaskel S, Sanchez C and Antonietti M 2010 *Adv. Funct. Mater.* **20** 1827-1833
[7]   Guo J H and Zhang H 2011 *Struct. Chem.* **22** 1039-1045
[8]   Badzian A R 1981 *Mat. Res. Bull.* **16** 1385-1393
[9]   Nakano S, Akaishi M, Sasaki T and Yamaoka S 1994 *Chem.Mater.* **6** 2246-2251
[10] Sasaki T, Akaishi M, Yamaoka S, Fujiki Y and Oikawa T 1993 *Chem. Mater.* **5** 695-699
[11] Solozhenko V L and Turkevich V Z 1997 *J. Am. Ceram. Soc.* **80** 3229–3232
[12] Nicolich J P, Ferdinand H, Brey G and Riedel R 2001 *J. Am. Ceram. Soc.* **84** 279-282
[13] Tian Y J, He J L, Yu D L, Li D C, Zou G T, Jia X P, Chen L X and Yanagisawa O 2002 *Radiat. Eff. Defect. S.* **157** 245-251
[14] Yang D P, Li Y A, Yang X X, Du Y H, Ji X R, Gong X L, Su Z P and Zhang T C 2007 *Chin. Phys. Lett.* **24** 1088-1091
[15] Li D, Yu D, Xu B, He J, Liu Z, Wang P and Tian Y 2008 *Cryst. Growth & Des.* **8** 2096-2100
[16] Tang M, He D, Wang W, Wang H, Xu C, Li F and Guan J 2012 *Scripta Mater.* **66** 781-784
[17] Filonenko V P, Khabashesku V N, Davydov V A, Zibrov I P and Agafonov V N 2008 *Inorg. Mater.* **44** 395-400
[18] Filonenko V P, Davydov V A, Zibrov I P, Agafonov V N and Khabashesku V N 2010 *Diam. Relat. Mater.* **19** 541-544
[19] Filonenko V P, Zibrov I P, Sidorov V A and Lyapin S G 2012 *Phase Transitions, Ordered States and New Materials* **3** 5
[20] Riedel R, Bill J and Passing G 1991 *Adv. Mater.* **3** 551-552
[21] Bill J, Riedel R and Passing G 1992 *Z. Anorg. allg. Chem.* **610** 83-90
[22] Decker D L 1971 *J. Appl. Phys.* **42** 3239-3244
[23] Khvostantsev L G, Sidorov V A and Tsiok O 1998 *Properties of Earth and Planetary Materials at High Pressure and Temperature* (*Geophysical Monograph* vol 101) ed M H Manghnani and T Yagi (Washington, DC: American Geophysical Union) p 89
[24] Girdini A and Tydings J E 1962 *Am. Mineral.* **47** 1393
[25] Matizamhuka W R, Sigalas I, Herrmann M, Dubronvinsky L, Dubrovinskaia N, Miyajima N, Mera G and Riedel R 2011 *Materials* **4** 2061-2072
[26] Hubacek M and Sato T 1995 *J. Solid State Chem.* **114** 258
[27] Watanabe M O, Itoh S, Mizushima K and Sasaki T 1996 *Appl. Phys. Lett.* **68** 2962-2964
[28] Watanabe M O, Sasaki T, Itoh S and Mizushima K 1996 *Thin Solid Films* **281/282** 334-336
[29] Marton D, Boyd K J, Al-Bayati A H, Todorov S S and Rabalais J W 1994 *Phys. Rev. Lett.* **73** 118-121